

Predicting *C. difficile* Infection Severity from the Taxonomic Composition of the Gut Microbiome

🔗 Kelly L. Sovacool¹, Sarah E. Tomkovich², Megan L. Coden³, Vincent B. Young^{2,4}, Krishna Rao⁴, and 🔗 Patrick D. Schloss^{2,5,†}

¹Department of Computational Medicine & Bioinformatics, University of Michigan

²Department of Microbiology & Immunology, University of Michigan

³Department of Molecular, Cellular, and Developmental Biology, University of Michigan

⁴Division of Infectious Diseases, Department of Internal Medicine, University of Michigan

⁵Center for Computational Medicine and Bioinformatics, University of Michigan

Compiled May 31, 2023

†Correspondence: pschloss@umich.edu.

1 **KEYWORDS:** *C. difficile* infection, supervised machine learning, gut microbiome, amplicon sequencing

INTRODUCTION

prevalence of cdi. prevalence of severe cdi outcomes.

Numerous studies indicate that the gut microbiome may play a role in *C. diff* colonization, infection, and clearance.

Contribution of the gut microbiome.

prediction models based on EHR for whether infection occurs in the first place already in use. so how about predicting

severity of infections to guide treatment? also models on EHR to predict adverse outcomes (Li, Rao). OTUs vs EHRs

to predict severity. CDI severity prediction models could be deployed to screen patients at risk and guide clinicians

to consider prescribing a different course of treatment. When paired with treatment options that may reduce risk of

severity, deploying prediction models can guide clinician decision-making to improve patient outcomes while minimizing

unnecessary harms.

A few ways to define CDI severity (Figure 1).

The IDSA definition is known to be a poor predictor of adverse outcomes (1), however, it is easy to collect.

new dataset.

Two goals: investigate whether we can predict CDI severity based on OTU data to inform how the gut microbiome may

modulate severity (ML-based science: good performance implies something about underlying biology), and determine

whether there is potential clinical value in OTU-based models.

RESULTS

Model performance We first set out to train the best models possible for each severity definition. Not all samples

have labels available for all four severity definitions due to missing data for some patient lab values and incomplete

chart review (Figure 1 B), thus each severity definition has a different number of samples (Table 1) when using as many

samples as possible. We refer to these as the full datasets. Random forest models were trained on repeated 100 splits

of the datasets into training and test sets, and performance was evaluated on the held-out test set using the area under

the receiver-operator characteristic curve (AUROC) the area under the balanced precision-recall curve (AUBPRC).

However, comparisons across these definitions is not fair when using different subsets of the data for each definition.

To better compare the model performances across different severity definitions, we selected the intersection of samples

(n=993) that had labels for all four severity definitions and repeated the model training and evaluation process.

Report median AUROC for training set and test set, and median AUBPRC for test set (Figure 2). Nearly all pairs of def-

TABLE 1 Sample counts and proportion of severe cases. Each severity definition has a different number of patient samples available, as well as a different proportion of cases labelled as severe.**(a)** Full datasets

	IDSA	Attributable	All-cause	Pragmatic
n	1,072.0	1,178.0	1,218.0	1,218.0
% Severe	34.2	2.2	7.1	5.4

(b) Intersection of samples with all labels available

	IDSA	Attributable	All-cause	Pragmatic
n	993.0	993.0	993.0	993.0
% Severe	32.7	2.6	4.6	2.6

initions have significantly different performances on the test set ($P < 0.05$) except for AUROC and AUBPRC of Attributable vs. Pragmatic on the intersection dataset (as they are identical), AUROC of Attributable vs. All-cause on the full dataset, and AUROC of Attributable vs. IDSA on the full dataset.

Feature importance We performed permutation feature importance to determine which OTUs contributed the most to model performance (Figure 3).

Estimating clinical value When considering the suitability of a model for deployment in clinical settings, the number needed to screen (NNS) is a highly relevant metric representing how many patients must be predicted as severe by the model to identify one true positive. We determined the decision threshold at the 95th percentile of risk for each prediction model and computed the confusion matrix and several performance metrics at this threshold including the NNS (Table 2). Among the models predicting severe outcomes, the models trained on the full datasets performed best with an NNS of 4 for the all-cause definition, 6 for the attributable definition, and 3 for the pragmatic definition. For context, prior studies predicted CDI-attributable severity using whole Electronic Health Record data and from a smaller set of 9 clinician-curated variables, achieving precision values of 0.417 (NNS = 2.4) for the EHR model and 0.17 (NNS = 6.0) for the curated model (2, 3). While the attributable definition had a worse NNS for our OTU-based models, it did not perform worse than prior curated models and it is the most clinically relevant as physician chart review ensures that positively-labelled severe outcomes are due to the CDI rather than other causes.

Even if a model performs well, it may not be useful in a clinical setting unless it can guide clinicians to choose between treatment options. At this time, we are not aware of any direct evidence that a particular treatment reduces the risk of severe CDI outcomes. However, with some assumptions we offer a proof-of-concept analysis of the potential clinical value of OTU-based severity prediction models. Paired with the NNS of these models,

Current clinical guidelines specify vancomycin and fidaxomicin as the standard antibiotics to treat CDI, with a preference for fidaxomicin due to its higher sustained resolution of CDI and reduced risk of recurrence (?). However, fidaxomicin is considerably more expensive than vancomycin, resulting in most CDI patients in the US being treated with vancomycin (TODO citation). If fidaxomicin were shown to reduce the risk of severe CDI outcomes, it could be preferen-

TABLE 2 Predictive model performance at 95th percentile of risk. The confusion matrix was computed for the decision threshold at the 95th percentile of risk for each severity prediction model, which corresponds to 5% of cases predicted to have a severe outcome. The number needed to screen (NNS) to identify one true positive is the reciprocal of precision.

(a) Full datasets

Outcome	Precision	NNS	Balanced Precision	Recall	Specificity	TP	FP	TN	FN
All-cause	0.25	4	0.81	0.18	0.96	3	9	217	14
Attributable	0.17	6	0.90	0.40	0.96	2	10	220	3
Pragmatic	0.33	3	0.90	0.31	0.97	4	8	222	9

(b) Intersection of samples with all labels available

Outcome	Precision	NNS	Balanced Precision	Recall	Specificity	TP	FP	TN	FN
All-cause	0.2	5	0.84	0.22	0.96	2	8	181	7
Attributable	0.1	10	0.81	0.20	0.95	1	9	184	4

tially prescribed to patients predicted to be at risk. While we are not aware of evidence demonstrating the superiority of fidaxomicin for reducing severe CDI outcomes,

$$\text{NNT} \times \text{NNS} = \text{NNB}$$

NNT for fidaxomicin, FMT, and/or Bezlotoxumab. Current standard is vancomycin because it's cheaper than fidaxomicin, even though IDSA recommends fidaxomicin.

rough estimate of costs. current: everyone gets vancomycin. potential: patients flagged as severe get fidaxomicin. based on NNB, estimate how much money saved in averting severe outcomes.

DISCUSSION

Performance

Discuss important OTUs. which ones concord with literature, which ones may be new. Abundance data are sparse, likely due to these patients being on antibiotics. Really showcases importance of having as many samples as possible when data are sparse and the outcome is low prevalence.

Compare to EHR-based models.

Models to guide treatment options. In the case of low-risk and non-invasive treatments such as choosing between oral antibiotics, a higher number of false positives may be tolerable as long as treatment cost is not unbearably high. However, for highly invasive and irreversibly treatments such as colectomy, false positives must be minimized. Cite studies saying fidaxomicin is cost-effective relative to vancomycin - mentioned by ?).

It's not enough for models to perform well to justify deploying them in a clinical setting; benefit over current practices

must be shown. Amplicon sequencing is not typically performed for CDI patients, but if there is clinical value to be gained by implementing OTU-based models, routinely sequencing and profiling the microbial communities of CDI patients could be justified.

MATERIALS AND METHODS

Sample collection This study was approved by the University of Michigan Institutional Review Board. All patient samples were collected by the University of Michigan Health System from January 2016 through December 2017. Stool samples that had unformed stool consistency were tested for *C. difficile* by the clinical microbiology lab with a two-step algorithm that included detection of *C. difficile* glutamate dehydrogenase and toxins A and B by enzyme immunoassay with reflex to PCR for the *tcdB* gene when results were discordant. 1,517 stool samples were collected from patients diagnosed with a CDI. Leftover stool samples that were sent to the clinical microbiology lab were collected and split into different aliquots. For 16S sequencing, the aliquot of stool was re-suspended in DNA genotek stabilization buffer and then stored in the -80°C freezer. Only the first CDI sample per patient was used for subsequent ML analyses such that no patient is represented more than once, resulting in a dataset of 1,277 samples.

16S rRNA gene amplicon sequencing Samples stored in DNA genotek buffer were thawed from the -80°C, vortexed, and then transferred to a 96-well bead beating plate for DNA extractions. DNA was extracted using the DNeasy Power-soil HTP 96 kit (Qiagen) and an EpMotion 5075 automated pipetting system (Eppendorf). The V4 region of the 16S rRNA gene was amplified with the AccuPrime Pfx DNA polymerase (Thermo Fisher Scientific) using custom barcoded primers, as previously described (4). Each library preparation plate for sequencing contained a negative control (water) and mock community control (ZymoBIOMICS microbial community DNA standards). The PCR amplicons were normalized (Sequal-Prep normalization plate kit from Thermo Fisher Scientific), pooled and quantified (KAPA library quantification kit from KAPA Biosystems), and sequenced with the MiSeq system (Illumina).

All sequences were processed with mothur (v1.46) using the MiSeq SOP protocol (5, 4). Paired sequencing reads were combined and aligned with the SILVA (v132) reference database (6) and taxonomy was assigned with a modified version of the Ribosomal Database Project reference sequences (v16) (7). Sequences were clustered into *de novo* OTUs with the OptiClust algorithm in mothur (8), resulting in 9,939 OTUs.

Defining CDI severity We explore four different ways to define CDI cases as severe or not. The IDSA definition of severe CDI is based on lab values collected on the day of diagnosis, with a case being severe if serum creatinine

level is greater than or equal to 1.5mgdL and the white blood cell count is greater than or equal to $15\text{k}\mu\text{L}$ (?). The remaining definitions focus on the occurrence of adverse outcomes, which may be more clinically relevant. The all-cause severity definition defines a case as severe if ICU admission, colectomy, or death occurs within 30 days of CDI diagnosis, regardless of the cause of the adverse event. The attributable severity definition is based on disease-related complications defined by the CDC, where an adverse event of ICU admission, colectomy, or death occurs within 30 days of CDI diagnosis, and the adverse event is determined to be attributable to the CDI by physician chart review (9). Finally, we defined a pragmatic severity definition that makes use of the attributable definition when available and falls back to the all-cause definition when chart review has not been completed, allowing us to use as many samples as we have available while taking physicians' expert opinions into account where possible.

Model training Random forest models were used to examine whether OTU data collected on the day of diagnosis could classify CDI cases as severe according to four different definitions of severity. We used the mikropml R package v1.5.0 (10) implemented in a custom version of the mikropml Snakemake workflow (11) for all steps of the machine learning analysis. We have full datasets which use all samples available for each severity definition, and an intersection dataset which consists of only the samples that have all four definitions labelled. The intersection dataset is the most fair for comparing model performance across definitions, while the full dataset allows us to use as much data as possible for model training and evaluation. Datasets were pre-processed with the default options in mikropml to remove features with near-zero variance and scale continuous features from -1 to 1. During pre-processing, 9,757 to 9,760 features were removed due to having near-zero variance, resulting in datasets ranging from 179 to 182 depending on the severity definition. No features had missing values and no features were perfectly correlated. We randomly split the data into an 80% training and 20% test set and repeated this 100 times, followed by training models with 5-fold cross-validation.

Model evaluation Model performance was calculated on the held-out test sets using the area under the receiver-operator characteristic curve (AUROC) and the area under the balanced precision-recall curve (AUBPRC). Permutation feature importance was then performed to determine which OTUs contributed most to model performance. We reported OTUs with a significant permutation test in at least 75 of the 100 models.

Since the severity labels are imbalanced with different frequencies of severity for each definition, we calculated balanced precision, the precision expected if the labels were balanced. The balanced precision and the area under the balanced precision-recall curve (AUBPRC) were calculated with Equations 1 and 7 from Wu et al. (12).

Code availability The complete workflow, code, and supporting files required to reproduce this manuscript with accompanying figures is available at <https://github.com/SchlossLab/severe-CDI>.

The workflow was defined with Snakemake (13) and dependencies were managed with conda environments. Scripts were written in R (14), Python (15), and GNU bash. Additional software and packages used in the creation of this manuscript include cowplot (16), ggtext (17), ggsankey (18), schtools (19), the tidyverse metapackage (20), Quarto, and vegan (21).

Data availability The 16S rRNA sequencing data have been deposited in the National Center for Biotechnology Information Sequence Read Archive (BioProject Accession no. PRJNA729511).

ACKNOWLEDGEMENTS

TODO

135 REFERENCES

1. **Stevens VW, Shoemaker HE, Jones MM, Jones BE, Nelson RE, Khader K, Samore MH, Rubin MA.** May 2020. Validation of the SHEA/IDSA Severity Criteria to Predict Poor Outcomes among Inpatients and Outpatients with *Clostridioides Difficile* Infection. *Infect Control & Hosp Epidemiol* 41 (5):510–516. doi:[10.1017/ice.2020.8](https://doi.org/10.1017/ice.2020.8).
2. **Li BY, Oh J, Young VB, Rao K, Wiens J.** May 2019. Using Machine Learning and the Electronic Health Record to Predict Complicated *Clostridium Difficile* Infection. *Open Forum Infect Dis* 6 (5):ofz186. doi:[10.1093/ofid/ofz186](https://doi.org/10.1093/ofid/ofz186).
3. **Rao K, Micic D, Natarajan M, Winters S, Kiel MJ, Walk ST, Santhosh K, Mogle JA, Galecki AT, LeBar W, Higgins PDR, Young VB, Aronoff DM.** Jul 2015. *Clostridium Difficile* Ribotype 027: Relationship to Age, Detectability of Toxins A or B in Stool With Rapid Testing, Severe Infection, and Mortality. *Clin Infect Dis* 61 (2):233–241. doi:[10.1093/cid/civ254](https://doi.org/10.1093/cid/civ254).
4. **Kozich JJ, Westcott SL, Baxter NT, Highlander SK, Schloss PD.** Sep 2013. Development of a Dual-Index Sequencing Strategy and Curation Pipeline for Analyzing Amplicon Sequence Data on the MiSeq Illumina Sequencing Platform. *Appl. Environ. Microbiol.* 79 (17):5112–5120. doi:[10.1128/AEM.01043-13](https://doi.org/10.1128/AEM.01043-13).
5. **Schloss PD, Westcott SL, Ryabin T, Hall JR, Hartmann M, Hollister EB, Lesniewski RA, Oakley BB, Parks DH, Robinson CJ, Sahl JW, Stres B, Thallinger GG, Van Horn DJ, Weber CF.** 2009. Introducing Mothur: Open-Source, Platform-Independent, Community-Supported Software for Describing and Comparing Microbial Communities. *Appl Environ Microbiol* 75 (23):7537–7541. doi:[10.1128/AEM.01541-09](https://doi.org/10.1128/AEM.01541-09).
6. **Quast C, Pruesse E, Yilmaz P, Gerken J, Schweer T, Yarza P, Peplies J, Glöckner FO.** Jan 2013. The SILVA Ribosomal RNA Gene Database Project: Improved Data Processing and Web-Based Tools. *Nucleic Acids Res* 41 (D1):D590–D596. doi:[10.1093/nar/gks1219](https://doi.org/10.1093/nar/gks1219).
7. **Cole JR, Wang Q, Fish JA, Chai B, McGarrell DM, Sun Y, Brown CT, Porras-Alfaro A, Kuske CR, Tiedje JM.** Jan 2014. Ribosomal Database Project: Data and Tools for High Throughput rRNA Analysis. *Nucl. Acids Res.* 42 (D1):D633–D642. doi:[10.1093/nar/gkt1244](https://doi.org/10.1093/nar/gkt1244).
8. **Westcott SL, Schloss PD.** Mar 2017. OptiClust, an Improved Method for Assigning Amplicon-Based Sequence Data to Operational Taxonomic Units. *mSphere* 2 (2):e00073–17. doi:[10.1128/mSphereDirect.00073-17](https://doi.org/10.1128/mSphereDirect.00073-17).
9. **McDonald LC, Coignard B, Dubberke E, Song X, Horan T, Kuttu PK.** 2007. Recommendations for Surveillance of *Clostridium Difficile*-Associated Disease. *Infect Control & Hosp Epidemiol* 28 (2):140–145. doi:[10.1086/511798](https://doi.org/10.1086/511798).
10. **Topçuoğlu BD, Lapp Z, Sovacool KL, Snitkin E, Wiens J, Schloss PD.** May 2021. Mikropml: User-Friendly R Package for Supervised Machine Learning Pipelines. *JOSS* 6 (61):3073. doi:[10.21105/joss.03073](https://doi.org/10.21105/joss.03073).
11. **Sovacool K, Lapp Z, Armour C, Lucas SK, Schloss P.** Jan. 2023. Mikropml Snakemake Workflow doi:[10.5281/zenodo.4759351](https://doi.org/10.5281/zenodo.4759351).
12. **Wu Y, Liu H, Li R, Sun S, Weile J, Roth FP.** Oct 2021. Improved Pathogenicity Prediction for Rare Human Missense Variants. *The Am J Hum Genet* 108 (10):1891–1906. doi:[10.1016/j.ajhg.2021.08.012](https://doi.org/10.1016/j.ajhg.2021.08.012).
13. **Köster J, Rahmann S.** Oct 2012. Snakemake — a Scalable Bioinformatics Workflow Engine. *Bioinformatics* 28 (19):2520–2522. doi:[10.1093/bioinformatics/bts480](https://doi.org/10.1093/bioinformatics/bts480).
14. **R Core Team.** 2020. R: A Language and Environment for Statistical Computing. R Foundation for Statistical Computing, Vienna, Austria.
15. **Van Rossum G, Drake FL.** 2009. Python 3 Reference Manual | Guide Books .
16. **Wilke CO.** 2020. Cowplot: Streamlined Plot Theme and Plot Annotations for 'Ggplot2'.
17. **Wilke CO.** 2020. Ggtext: Improved Text Rendering Support for 'Ggplot2'.
18. **Sjoberg D.** 2022. Ggsankey: Sankey, Alluvial and Sankey Bump Plots.

19. **Sovacool K, Lesniak N, Schloss P.** 2022. Schtools: Schloss Lab Tools for Reproducible Microbiome Research doi:[10.5281/zenodo.6540687](https://doi.org/10.5281/zenodo.6540687).
20. **Wickham H, Averick M, Bryan J, Chang W, McGowan LD, François R, Golemund G, Hayes A, Henry L, Hester J, Kuhn M, Pedersen TL, Miller E, Bache SM, Müller K, Ooms J, Robinson D, Seidel DP, Spinu V, Takahashi K, Vaughan D, Wilke C, Woo K, Yutani H.** Nov 2019. Welcome to the Tidyverse. *J Open Source Softw* 4 (43):1686. doi:[10.21105/joss.01686](https://doi.org/10.21105/joss.01686).
21. **Oksanen J, Simpson GL, Blanchet FG, Kindt R, Legendre P, Minchin PR, O'Hara RB, Solymos P, Stevens MHH, Szoecs E, Wagner H, Barbour M, Bedward M, Bolker B, Borcard D, Carvalho G, Chirico M, Caceres MD, Durand S, Evangelista HBA, FitzJohn R, Friendly M, Furneaux B, Hannigan G, Hill MO, Lahti L, McGlinn D, Ouellette MH, Cunha ER, Smith T, Stier A, Braak CJFT, Weedon J.** 2023. *Vegan: Community Ecology Package*.

136 **FIGURES**

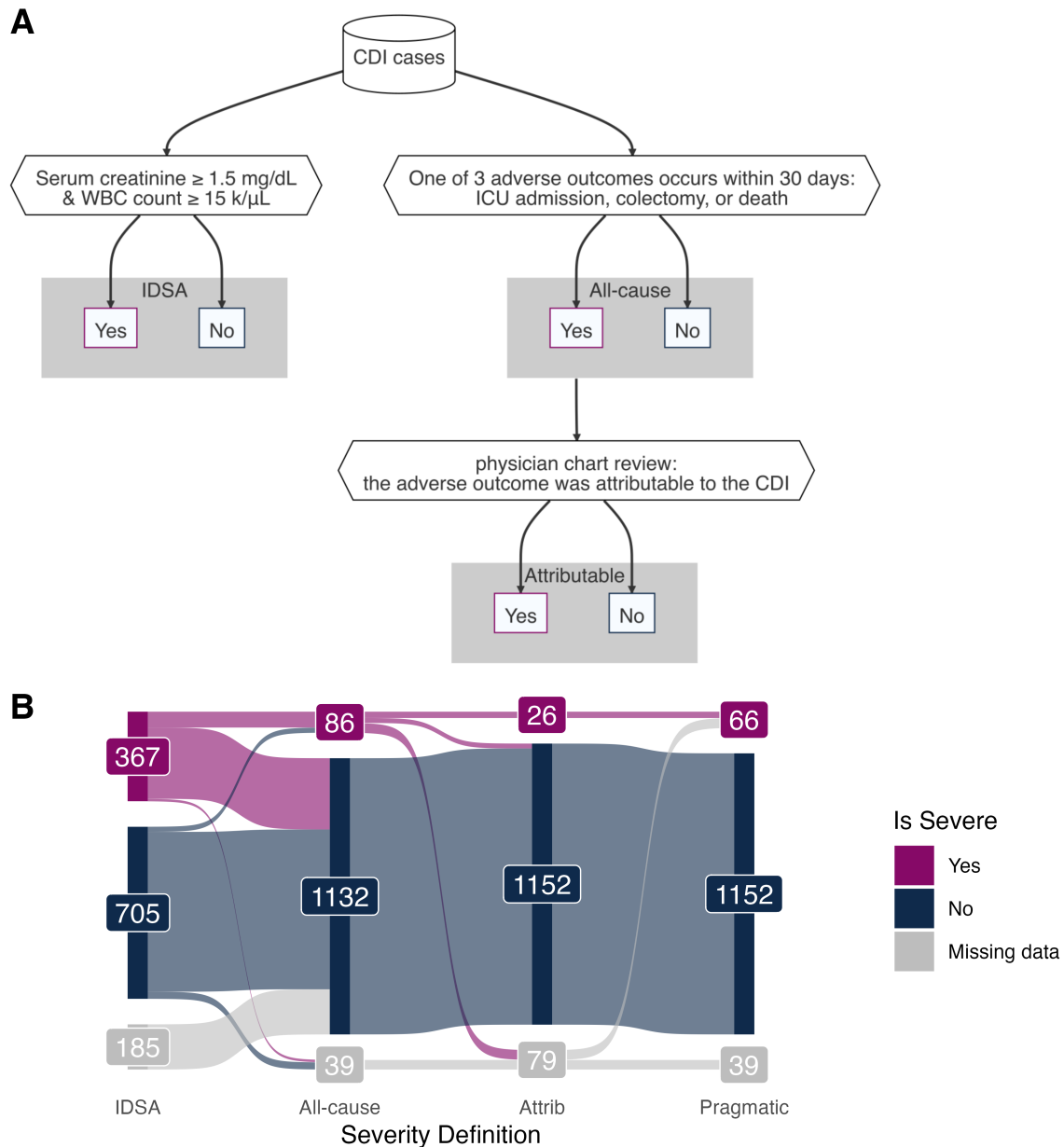


FIG 1 CDI severity definitions. A) Decision flow chart to define CDI cases as severe according to the Infectious Diseases Society of America (IDSA) based on lab values, the occurrence of an adverse outcome due to any cause (All-cause), and the occurrence of disease-related complications confirmed as attributable to CDI with chart review (Attributable). **B)** The proportion of severe CDI cases labelled according to each definition. An additional 'Pragmatic' severity definition uses the Attributable definition when possible, and falls back to the All-cause definition when chart review is not available.

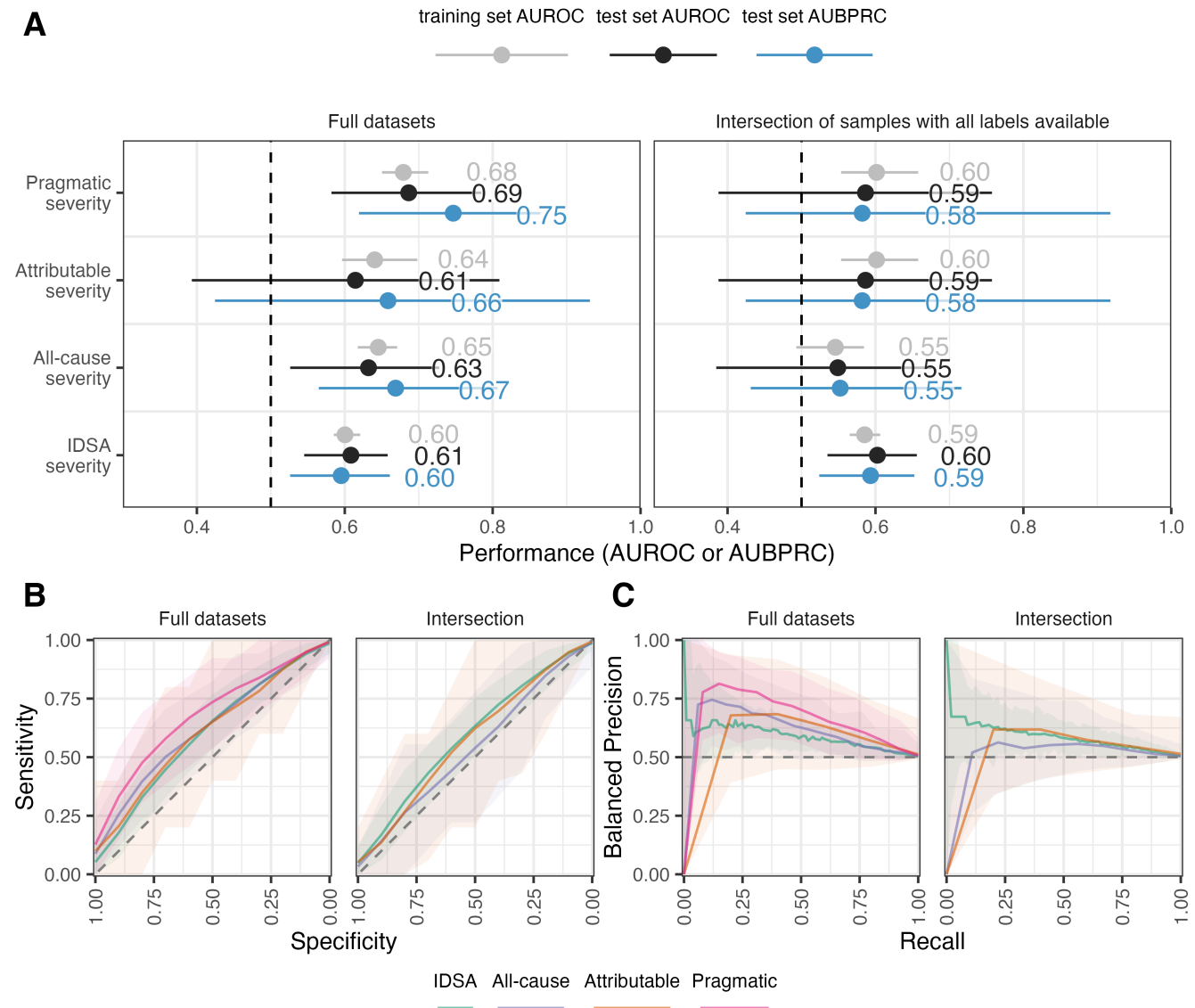


FIG 2 Performance of ML models. In the left panels, models were trained on the full dataset, with different numbers of samples available for each severity definition. In the right panels, models were trained on the intersection of samples with all labels available for each definition. Note that the intersection dataset for Attributable and Pragmatic severity have exactly the same labels, thus identical values are expected. **A)** Area under the receiver-operator characteristic curve (AUROC) for the test sets and cross-validation folds of the training sets, and the area under the balanced precision-recall curve (AUBPRC) for the test sets. Each point is the median performance across 100 train/test splits with tails as the 95% CI. Nearly all pairs of definitions have significantly different performances on the test set ($P < 0.05$) except for AUROC and AUBPRC of Attributable vs. Pragmatic on the intersection dataset (as they are identical), AUROC of Attributable vs. All-cause on the full dataset, and AUROC of Attributable vs. IDSA on the full dataset. **B)** Receiver-operator characteristic curves for the test sets. Mean specificity is reported at each sensitivity value, with ribbons as the 95% CI. **C)** Balanced precision-recall curves for the test sets. Mean balanced precision is reported at each recall value, with ribbons as the 95% CI.

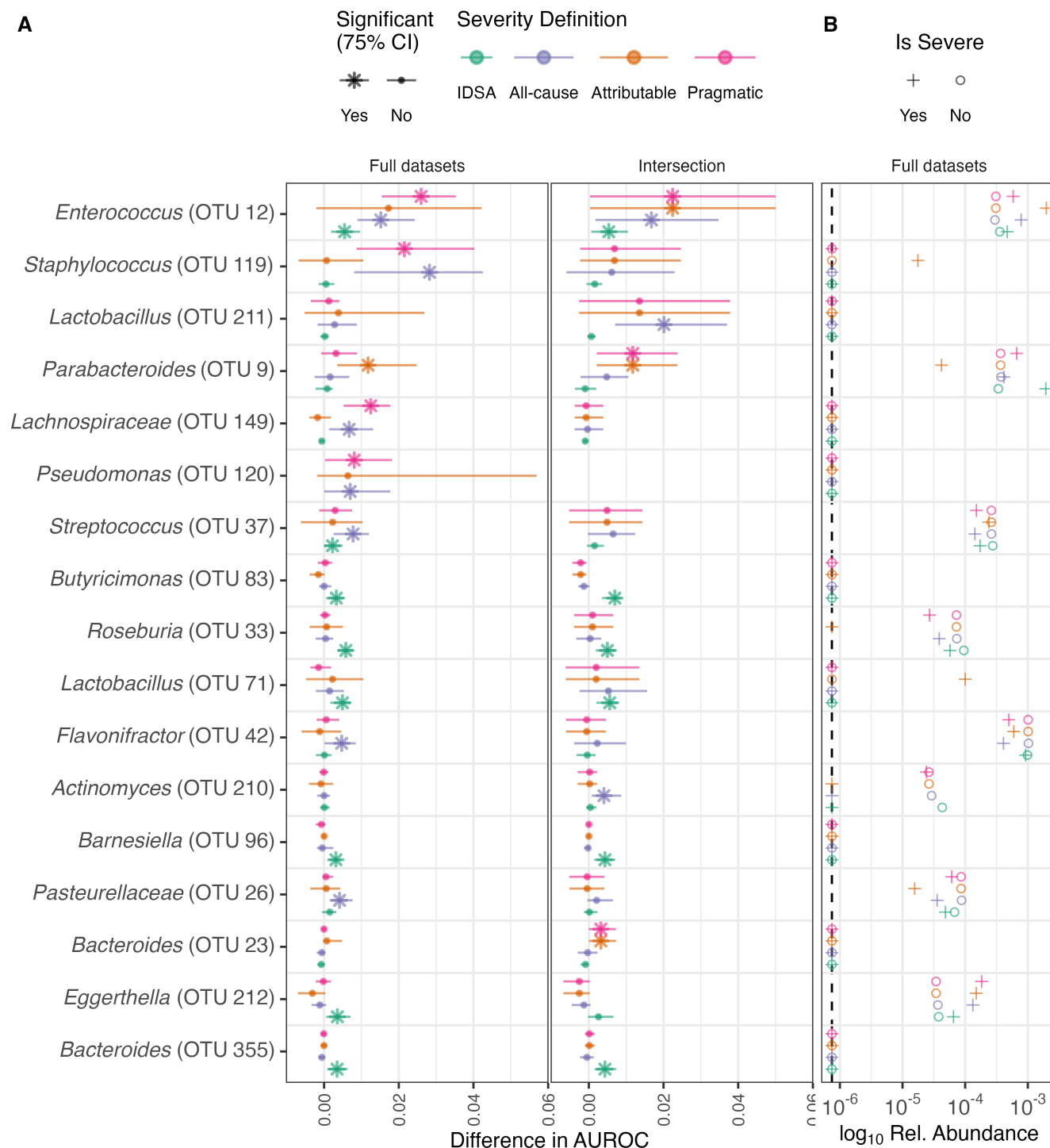


FIG 3 Feature importance. A) Feature importance via permutation test. For each OTU, the order of samples was randomized in the test set 100 times and the performance was re-calculated to estimate the permutation performance. An OTU was considered important if the performance decreased when the OTU was permuted in at least 75% of the models. OTUs with a greater difference in AUROC (actual performance minus permutation performance) are more important. Left: models were trained on the full datasets, with different numbers of samples available for each severity definition. Right: models were trained on the intersection of samples with all labels available for each definition. Note that Attributable and Pragmatic severity are exactly the same for the intersection dataset. *Pseudomonas* (OTU 120) is not shown for IDSA severity in the full datasets nor in the intersection dataset because it was removed during pre-processing due to having near-zero variance. **B)** Log₁₀-transformed median relative abundances of the most important OTUs on the full datasets, grouped by severity (shape). The vertical dashed line is the limit of detection.